NUREG/CR-1232

A Three-Dimensional Fluid Finite Element

Manuscript Completed: July 1979
Date Published: February 1980

Prepared by
K. J. Bathe, W. F. Hahn

Massachusetts Institute of Technology
Cambridge, MA 02139

Prepared for
Division of Project Management
Office of Nuclear Reactor Regulation
U.S. Nuclear Regulatory Commission
Washington, D.C. 20555
NRC Contract No. NRC 0378-142

ABSTRACT

A three-dimensional fluid finite element compatible with the solid elements in the ADINA finite element program has been developed for the analysis of wave propagation in fluid and fluid-structural systems. The fluid element can model inviscid compressible fluids with constant bulk modulus. Although the final discretized equations of motion are valid for general loading and displacement conditions, the numerical computations only admit relatively small fluid displacements unless mesh rezoning would be used.

ACKNOWLEDGEMENT

The work presented in this report was sponsored by the U.S. Nuclear Regulatory Commission under Contract No. NRC0378-142 with the Massachusetts Institute of Technology.

Work at the Institute was conducted under the direction of K.J. Bathe, Associate Professor of Mechanical Engineering. Mr. V. Sonnad, Research Assistant, assisted in the development and implementation of the fluid element.

TABLE OF CONTENTS

The following paper documents the theory used in the formulation of the fluid element.

Computers & Structures Vol. 10, pp. 383–391
0045-7949/79/0401-0383/$02.00/0

ON TRANSIENT ANALYSIS OF FLUID-STRUCTURE SYSTEMS

K. J. BATHE and W. F. HAHN
Department of Mechanical Engineering, Massachusetts Institute of Technology, Cambridge, MA 02139, U.S.A.

(Received 12 May 1978)

Abstract—Finite element procedures for the dynamic analysis of fluid-structure systems are presented and evaluated. The fluid is assumed to be inviscid and compressible and is described using an updated Lagrangian formulation. Variable-number-nodes isoparametric two- and three-dimensional elements with lumped or consistent mass idealization are employed in the finite element discretization, and the incremental dynamic equilibrium equations are solved using explicit or implicit time integration. The solution procedures are applied to the analysis of a number of fluid-structure problems including the nonlinear transient analysis of a pipe test.

1. INTRODUCTION

The accurate and efficient transient analysis of fluid-structure problems has during recent years attracted much research effort[1–5]. Fluid-structure problems need to be considered in various engineering disciplines, and to a great deal in reactor safety deliberations[1]. In this paper we consider the response of fluid-structure systems in which the fluid can be idealized as being inviscid and compressible, and we focus particular attention on the analysis of problems in which the fluid transmits a significant amount of energy in a relatively short time duration (such as might occur under accident conditions).

An obvious approximate procedure to analyze a fluid-structure problem is to perform the complete analysis in two steps: first, the fluid response is calculated assuming that the structure is rigid; and then the structural response is predicted that is due to the calculated fluid pressures. In most cases this analysis approach will (probably) yield a conservative estimate of the structural deformations. Thus, a drawback of this decoupling of the fluid and the structural analysis is that a substantial overdesign may be reached. On the other hand, this procedure of analysis may yield an unsound design if significant resonance between the fluid and the structure occurs.

A decoupled analysis of the fluid and the structural response is somewhat a natural engineering solution, because, historically, finite difference analysis procedures are employed for analysis of fluid response and finite element procedures are used for structural analysis. Thus, it is natural to employ a finite difference-based computer program to perform the fluid analysis and a finite element program to predict the structural response.

Recognizing the serious deficiency of a decoupled analysis, emphasis has been directed in recent years towards the development of solution algorithms that can be employed to directly analyze the coupled response of fluid-structure systems. In the search for effective solution procedures the versatility and generality of the finite element method for structural analysis and the close relationship between finite difference and finite element procedures suggest that it be very effective to include fluid elements in the finite element programs. These elements can then be directly employed together with structural elements to model fluid-structure systems. At present, some solution capabilities are available, but the programs use only lower-order fluid elements, are restricted to two-dimensional analysis, and, in general, lack versatility with regard to explicit and implicit time integration and lumped and consistent mass idealizations[1].

The objective of this paper is to report on our recent developments of solution capabilities for fluid-structure interaction problems. In the paper, first the Lagrangian formulation of the inviscid and compressible variable-number-nodes 3–8 two-dimensional and 4–21 three-dimensional isoparametric fluid elements is briefly summarized[6]. These elements have been implemented in the computer program ADINA[7]. The elements can undergo large displacements, they can be employed with implicit (Newmark or Wilson-θ methods) or explicit (central difference method) time integration schemes, and lumped or consistent mass idealizations. Next, the elements, time integration schemes and modeling considerations that lead to either a lumped or consistent mass idealization are discussed. Finally, a number of demonstrative sample solutions are presented. Here, the analysis of a fluid pressure pulse propagating in a pipe section and leading to elastic–plastic structural response is discussed in detail with regard to the finite element modeling and the time integration scheme employed.

2. CALCULATION OF FLUID FINITE ELEMENTS

The objective in this work was to develop a fluid-structure analysis capability that can be employed in the analysis of problems in which no gross fluid motion occurs. For these types of problems a Lagrangian formulation is effective. The fluid elements can then be employed in conjunction with structural elements that are also based on Lagrangian descriptions. The following two basic assumptions have been used in the formulation of the fluid elements:

1. The fluid is compressible and inviscid.
2. Interaction between mechanical and thermal processes is negligible; thus only the mechanical equations are needed to describe the fluid response.

Using a Lagrangian formulation, in principle, a total or updated Lagrangian formulation can be employed, but considering the numerical operations required for fluid systems, an updated Lagrangian (U.L.) formulation is more effective[8].

2.1 *Continuum mechanics formulation*

Consider a body of fluid undergoing large deformations and assume that the solutions are known at all discrete time points $0, \Delta t, 2\Delta t, \ldots t$. The basic aim of the formulation is to establish an equation of virtual work from which the unknown static and kinematic variables in the configuration at time $t+\Delta t$ can be solved. Since the displacement-based finite element procedure shall be employed for numerical solution, we use the principle of virtual displacements to express the equilibrium of the fluid body. In explicit time integration equilibrium is considered at time t [6]

$$\int_{{}^tV} -{}^tp\,\delta_t e_{ii}\,{}^t dv = {}^t\mathcal{R} \tag{1}$$

whereas in implicit time integration equilibrium is considered at time $t+\Delta t$,

$$\int_{{}^{t+\Delta t}V} -{}^{t+\Delta t}p\,\delta_{t+\Delta t}e_{ii}\,{}^{t+\Delta t}dv = {}^{t+\Delta t}\mathcal{R}. \tag{2}$$

In eqn (1) ${}^tp$ is the pressure at time t, $\delta_t e_{ii}$ is a virtual variation of the volumetric strain at time t,

$$\delta_t e_{ii} = \delta \frac{\partial u_i}{\partial {}^t x_i} \quad (\text{sum on } i) \tag{3}$$

${}^tV$ is the volume at time t and ${}^t\mathcal{R}$ is the external virtual work corresponding to time t, and includes the effect of body, surface and inertial forces [8]. The quantities in eqn (2) are defined analogously.

Equations (1) and (2) contain the momentum balance and continuity equations used in analytical fluid mechanics [9]. In addition we also use the constitutive relation

$${}^tp = -{}^t\alpha\,\Delta V/V_0 \tag{4}$$

where ΔV is the total volume change of a differential volume V_0 and ${}^t\alpha$ is a variable that may be pressure dependent. Using eqn (4) we can directly employ eqn (1) in transient analysis. For static analysis or implicit time integration we linearize eqn (2) as summarized in Table 1 and obtain [8, 9],

$$\int_{{}^tV} {}^t\kappa\,{}_te_{ii}\,\delta_t e_{ii}\,{}^tdv - \int_{{}^tV} {}^tp\,\delta_t\eta_{ii}\,{}^tdv = {}^{t+\Delta t}\mathcal{R} + \int_{{}^tV} {}^tp\,\delta_t e_{ii}\,{}^tdv \tag{5}$$

where ${}^tp$ is evaluated using eqn (4) and ${}^t\kappa$ is the tangent fluid bulk modulus.

The linearization used to arrive at eqn (5) introduces errors in the solution which may be large if the time step is relatively large. In order to reduce solution errors and in some cases instabilities (see sample problem 4.4) equilibrium iterations are used. In this case, we employ the following equation to solve for the incremental displacements [10]

$$\int_{{}^tV} {}^t\kappa\,\Delta_t e_{ii}^{(k)}\,\delta_t e_{ii}\,{}^tdv - \int_{{}^tV} {}^tp\,\delta\Delta_t\eta_{ii}^{(k)}\,{}^tdv$$
$$= {}^{t+\Delta t}\mathcal{R} + \int_{{}^{t+\Delta t}V^{(k-1)}} {}^{t+\Delta t}p^{(k-1)}\,\delta_{t+\Delta t}e_{ii}^{(k-1)}\,{}^{t+\Delta t}dv^{(k-1)}$$
$$k = 1, 2, \ldots \tag{6}$$

where

$${}^{t+\Delta t}u_i^{(k)} = {}^{t+\Delta t}u_i^{(k-1)} + \Delta u_i^{(k)}$$

and eqn (6) reduces to eqn (5) when $k=1$.

Table 1. Updated Lagrangian formulation of fluid elements

1. *Equation of motion*

$$\int_{{}^{t+\Delta t}V} -{}^{t+\Delta t}p\,\delta_{t+\Delta t}e_{ii}\,{}^{t+\Delta t}dv = {}^{t+\Delta t}\mathcal{R}$$

or

$$\int_{{}^tV} {}^{t+\Delta t}_{\ t}S_{ij}\,\delta\,{}^{t+\Delta t}_{\ t}\epsilon_{ij}\,{}^tdv = {}^{t+\Delta t}\mathcal{R}$$

where

$${}^{t+\Delta t}_{\ t}S_{ij} = \frac{{}^t\rho}{{}^{t+\Delta t}\rho}\,{}_{t+\Delta t}^{\ \ t}x_{i,r} - {}^{t+\Delta t}p_{t+\Delta t}{}^tx_{j,r};$$

$$\delta\,{}^{t+\Delta t}_{\ t}\epsilon_{ij} = \delta\frac{1}{2}({}_tu_{i,j} + {}_tu_{j,i} + {}_tu_{k,i}\,{}_tu_{k,j})$$

2. *Incremental decompositions*

(a) Stresses

$${}^{t+\Delta t}_{\ t}S_{ij} = -{}^tp\,\delta_{ij} + {}_tS_{ij};\quad \delta_{ij} = \text{Kronecker delta}.$$

(b) Strains

$${}^{t+\Delta t}_{\ t}\epsilon_{ij} = {}_t\epsilon_{ij};\quad {}_t\epsilon_{ij} = {}_te_{ij} + {}_t\eta_{ij}$$

$${}_te_{ij} = \frac{1}{2}({}_tu_{i,j} + {}_tu_{j,i});\ {}_t\eta_{ij} = \frac{1}{2}\,{}_tu_{k,i}\,{}_tu_{k,j}$$

3. *Equation of motion with incremental decompositions*

Substituting from (a) and (b) into the equation of motion we obtain

$$\int_{{}^tV} {}_tS_{ij}\,\delta_t\epsilon_{ij}\,{}^tdv - \int_{{}^tV} {}^tp\,\delta_t\eta_{ii}\,{}^tdv = {}^{t+\Delta t}\mathcal{R} + \int_{{}^tV} {}^tp\,\delta_t e_{ii}\,{}^tdv.$$

4. *Linearization of equation of motion*

Using the approximations ${}_tS_{ij} = {}^t\kappa\,e_{ii}\delta_{ij}$, $\delta_t\epsilon_{ij} = \delta_t e_{ij}$ we obtain an approximate equation of motion

$$\int_{{}^tV} {}^t\kappa\,{}_te_{ii}\,\delta_t e_{ii}\,{}^tdv - \int_{{}^tV} {}^tp\,\delta_t\eta_{ii}\,{}^tdv = {}^{t+\Delta t}\mathcal{R} + \int_{{}^tV} {}^tp\,\delta_t e_{ii}\,{}^tdv.$$

2.2 *Finite element discretization*

Using isoparametric finite element discretization, the basic assumptions for an element are [6]

$${}^tx_i = \sum_{k=1}^{N} h_k\,{}^tx_i^k$$
$${}^tu_i = \sum_{k=1}^{N} h_k\,{}^tu_i^k \qquad i = 1,2,3 \text{ depending on one, two or three-dimensional analysis, respectively} \tag{7}$$
$$\Delta u_i = \sum_{k=1}^{N} h_k\,\Delta u_i^k$$

where N is the number of nodes of the element considered, the h_k are the element interpolation functions, and the ${}^tx_i^k$, ${}^tu_i^k$ and Δu_i^k are the coordinates, displacements and incremental displacements of nodal point k at time t.

Substituting the relations in eqn (7) into eqns (1) and (6) and including the effect of inertia forces, we obtain the governing finite element equations in explicit time integration,

$$\mathbf{M}\,{}^t\ddot{\mathbf{u}} = {}^t\mathbf{R} - {}^t_t\mathbf{F} \tag{8}$$

and in implicit time integration

$$\mathbf{M}\,{}^{t+\Delta t}\ddot{\mathbf{u}}^{(i)} + ({}^t_t\mathbf{K}_L + {}^t_t\mathbf{K}_{NL})\Delta\mathbf{u}^{(i)} = {}^{t+\Delta t}\mathbf{R} - {}^{t+\Delta t}_{t+\Delta t}\mathbf{F}^{(i-1)} \tag{9}$$

POOR ORIGINAL

where the first iteration, $i = 1$, corresponds to the solution of eqn (5).

In eqns (8) and (9) we have

$\mathbf{M}$ = time independent lumped or consistent mass matrix

${}^t_t\mathbf{K}_L, {}^t_t\mathbf{K}_{NL}$ = linear, nonlinear strain (tangent) stiffness matrix in the configuration at time t

${}^t\ddot{\mathbf{u}}, {}^{t+\Delta t}\ddot{\mathbf{u}}$ = vector of nodal point accelerations in the configuration at time $t, t+\Delta t$

$\Delta\mathbf{u}$ = vector of incremental nodal point displacements

${}^t\mathbf{R}, {}^{t+\Delta t}\mathbf{R}$ = vector of external loads at time $t, t+\Delta t$

${}^t_t\mathbf{F}, {}^{t+\Delta t}_{t+\Delta t}\mathbf{F}$ = vector of nodal point forces at time $t, t+\Delta t$ and

the superscript (i) indicates ith iteration.

The matrices in eqns (8) and (9) are defined in Table 2 for a single element using the following notation:

$\mathbf{H}$ = displacement transformation matrix

$\mathbf{H}^S$ = surface displacement transformation matrix

${}^t_t\mathbf{V}$ = dilatation-displacement transformation matrix

${}^t_t\mathbf{B}_{NL}$ = nonlinear strain-displacement transformation matrix

${}^{t+\Delta t}_{0}\mathbf{t}, {}^{t+\Delta t}_{0}\mathbf{f}$ = traction and body force vectors.

The displacement transformation matrices and force vectors are defined as usual[6, 10], and Table 3 gives the matrices ${}^t_t\mathbf{V}$ and ${}^t_t\mathbf{B}_{NK}$ for the two and three dimensional fluid elements.

Using the above formulation, the 4–8 and 8–21 variable-number nodes elements (shown in Fig. 1[6]) with lumped or consistent mass assumptions have been implemented in ADINA for two- and three-dimensional analysis, respectively. The lumped mass matrix of an element is calculated by simply allocating 1/N times the total element mass (where N = number of nodes) to the nodal degrees of freedom.

We may note that the continuum mechanics equations of motion (eqns 1 and 2) are valid for general displacements. However, considering the finite element equations of motion severe mesh distortions that are due to large displacements reduce the accuracy of a finite element solution. In order to preserve solution accuracy rezoning would have to be used which is not considered in this study.

Table 2. Finite element matrices

Integral	Matrix evaluation
$\int_{^0v} {}^0\rho\, {}^{t+\Delta t}\ddot{u}_k \delta u_k\, {}^0dv$	$\mathbf{M}\,{}^{t+\Delta t}\ddot{\mathbf{u}} = {}^0\rho \left(\int_{^0v} \mathbf{H}^T \mathbf{H}\, {}^0dv\right) {}^{t+\Delta t}\ddot{\mathbf{u}}$ (consistent mass)
${}^{t+\Delta t}\mathcal{R} = \int_{^0A} {}^{t+\Delta t}_{0}t_k \delta u_k\, {}^0da + \int_{^0v} {}^0\rho\, {}^{t+\Delta t}_{0}f_k \delta u_k\, {}^0dv$	${}^{t+\Delta t}\mathbf{R} = \int_{^0A} \mathbf{H}^{ST}\, {}^{t+\Delta t}_{0}\mathbf{t}\, {}^0da + {}^0\rho \int_{^0v} \mathbf{H}^T\, {}^{t+\Delta t}_{0}\mathbf{f}\, {}^0dv$
$\int_{^tv} {}^t\kappa\, {}_te_{ii}\, \delta\, {}_te_{jj}\, {}^tdv$	${}^t_t\mathbf{K}_L \mathbf{u} = \left(\int_{^tv} {}^t\kappa\, {}^t_t\mathbf{V}^T\, {}^t_t\mathbf{V}\, {}^tdv\right)\mathbf{u}$
$\int_{^tv} -{}^tp\, \delta\, {}_t\eta_{ii}\, {}^tdv$	${}^t_t\mathbf{K}_{NL}\mathbf{u} = \left(\int_{^tv} -{}^tp\, {}^t_t\mathbf{B}^T_{NL}\, {}^t_t\mathbf{B}_{NL}\, {}^tdv\right)\mathbf{u}$
$\int_{^tv} -{}^tp\, \delta\, {}_te_{ii}\, {}^tdv$	${}^t_t\mathbf{F} = \int_{^tv} -{}^tp\, {}^t_t\mathbf{V}^{T\,t}dv$

Table 3. Linear and nonlinear strain-displacement transformation matrices

Two-dimensional analysis

Dilatation-displacement transformation vector:

$$ {}^t_t\mathbf{V} = \left[\left({}_th_{1,1} + \frac{h_1}{{}^t\bar{x}_1}\right) {}_th_{1,2} \left({}_th_{2,1} + \frac{h_2}{{}^t\bar{x}_1}\right) \cdots \left({}_th_{N,1} + \frac{h_N}{{}^t\bar{x}_1}\right) {}_th_{N,2}\right] $$

where

$$ {}^t\bar{x}_1 = \sum_{i=1}^{N} h_i\, {}^tx_1^i. $$

Nonlinear strain-displacement transformation matrix:

$$ {}^t_t\mathbf{B}_{NL} = \begin{bmatrix} {}_th_{1,1} & 0 & {}_th_{2,1} & \cdots & {}_th_{N,1} & 0 \\ {}_th_{1,2} & 0 & {}_th_{2,2} & \cdots & {}_th_{N,2} & 0 \\ 0 & {}_th_{1,1} & 0 & \cdots & 0 & {}_th_{N,1} \\ 0 & {}_th_{1,2} & 0 & \cdots & 0 & {}_th_{N,2} \\ \frac{h_1}{{}^t\bar{x}_1} & 0 & \frac{h_2}{{}^t\bar{x}_1} & \cdots & \frac{h_N}{{}^t\bar{x}_1} & 0 \end{bmatrix} $$

$\left(\frac{h_i}{{}^t\bar{x}_1}\right.$ is included only in axisymmetric analysis$\left.\right)$

Three-dimensional analysis

Dilatation-displacement transformation vector

$$ {}^t_t\mathbf{V} = [{}_th_{1,1}\,{}_th_{1,2}\,{}_th_{1,3}\,{}_th_{2,1} \cdots {}_th_{N,1}\,{}_th_{N,2}\,{}_th_{N,3}]. $$

Nonlinear strain-displacement transformation matrix:

$$ {}^t_t\mathbf{B}_{NL} = \begin{bmatrix} {}^t_t\bar{\mathbf{B}}_{NL} & \mathbf{0} & \mathbf{0} \\ \mathbf{0} & {}^t_t\bar{\mathbf{B}}_{NL} & \mathbf{0} \\ \mathbf{0} & \mathbf{0} & {}^t_t\bar{\mathbf{B}}_{NL} \end{bmatrix}; \quad \mathbf{0} = \begin{bmatrix} 0 \\ 0 \\ 0 \end{bmatrix} $$

$$ {}^t_t\bar{\mathbf{B}}_{NL} = \begin{bmatrix} {}_th_{1,1} & 0 & 0 & {}_th_{2,1} & 0 & 0 & \cdots & {}_th_{N,1} \\ th_{1,2} & 0 & 0 & {}_th_{2,2} & 0 & 0 & \cdots & {}_th_{N,2} \\ {}_th_{1,3} & 0 & 0 & {}_th_{2,3} & 0 & 0 & \cdots & {}_th_{N,3} \end{bmatrix} $$

2.3 *Analysis of fluid finite elements*

The variable-number-nodes fluid elements shown in Fig. 1 are compatible with the solid elements available in ADINA. This compatibility is important because higher-order isoparametric solid elements have proven to be significantly more effective than lower-order elements in analysis of problems with significant bending response and would naturally be employed with high-order fluid elements. However, to model the complete fluid domain appropriately, the basic characteristics of the fluid elements need to be known.

The basic characteristics of a fluid element are displayed by the element eigenvalues and eigenvectors[6]. Figure 2 summarizes the eigensystem of a 4-node two-dimensional element. The figure shows that, as reported earlier, using reduced Gauss integration (1 point integration) for the 4-node element the hourglass patterns correspond to zero eigenvalues. Various attempts have been made to remove the instability of the hourglass deformation modes without increasing the computational expense significantly, but it is believed to be best to use 2×2 Gauss integration. Indeed, the formulation-consistent removal of the hourglass instability using 2×2

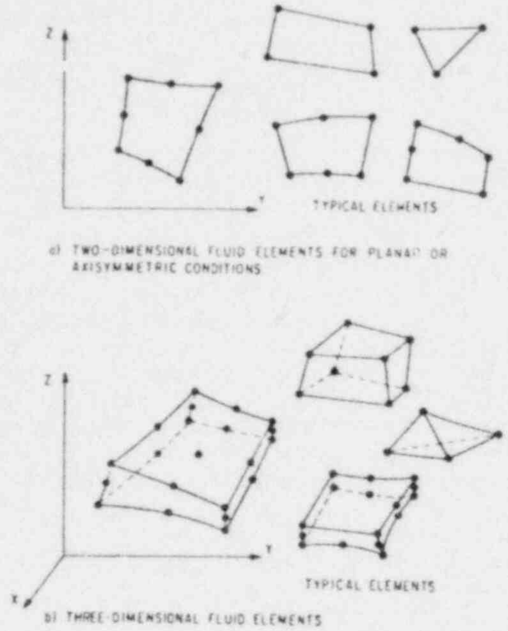

Fig. 1. Fluid elements in ADINA.

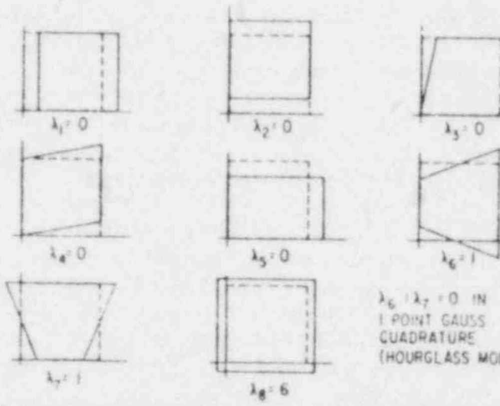

(a) EIGENVALUES AND EIGENVECTORS OF 4-NODE TWO-DIMENSIONAL PLANE FLUID ELEMENT, EXACT INTEGRATION

INTEGRATION ORDER	NO. OF ZERO EIGENVALUES / NO. OF dof			
	TWO-DIMENSIONAL		THREE-DIMENSIONAL	
	4-NODE	8-NODE	8-NODE	20-NODE
2 x 2	5/8	12/16	17/24	52/60
3 x 3		10/16		43/60

(b) NUMBER OF ZERO STRAIN ENERGY MODES FOR FLUID ELEMENTS (INCLUDING RIGID BODY MODES)

Fig. 2. Eigensystems of two and three-dimensional fluid elements.

Gauss quadrature is an advantage of a finite element formulation over a finite difference analysis.

Figure 2 also gives the number of zero eigenvalues of the 8-node two-dimensional and 8 and 20-node three-dimensional elements. As for the 4-node two-dimensional element, reduced integration introduces additional zero eigenvalues that can result in solution instabilities in the analysis of a fluid-structure system.

Of particular interest is the analysis of fluid-filled pipes. If the geometry and loading are axisymmetric, these fluid-structure systems can be modeled using the axisymmetric elements, and the question is whether higher or lower-order elements should be employed. It is well-known that in axisymmetric analysis of solids, higher-order isoparametric elements need be employed for accurate prediction of stresses. The same conclusion is reached for the fluid elements. Figure 3 shows the stresses calculated in axisymmetric plane strain fluid-solid models with a varying bulk modulus in the fluid and compares the results with theoretical values.

The use of higher-order fluid and solid elements in transient analysis requires that a distinct choice be made on the use of a lumped or consistent mass idealization. If 4-node two-dimensional elements (and 8-node three-dimensional elements) are employed it is probably most effective to use a lumped mass model. Not only is the computational expense less when using a lumped mass matrix but the similarity between the finite element equations and the finite difference equations (in some cases these are the equations used in the method of characteristics) requires the use of a lumped mass matrix for best solution accuracy[11]. On the other hand,

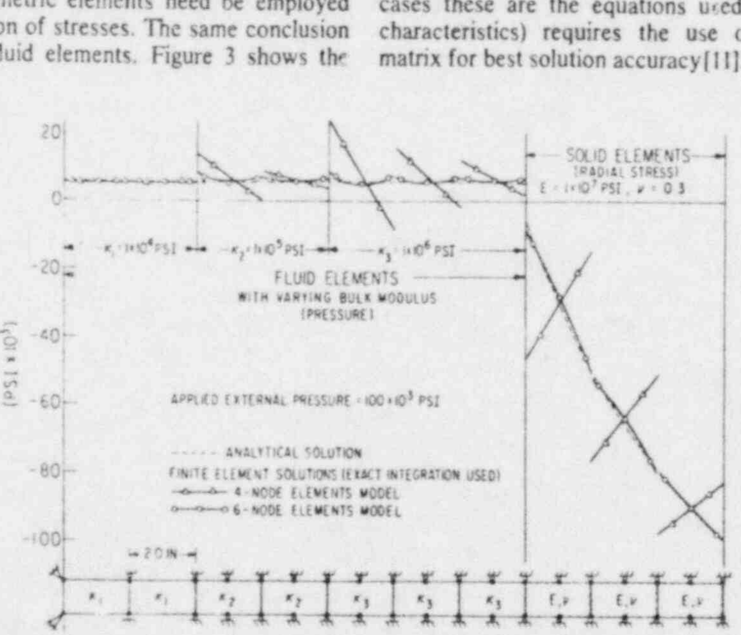

Fig. 3. Analysis of axisymmetric plane strain fluid-structure model, 4-node vs 6-node elements.

POOR ORIGINAL

considering the use of higher-order elements, a lumped mass characterization leads to spurious oscillations that arise because a lumped mass distribution does not represent a consistent loading on the elements. Since it is the objective to employ as few higher-order elements as possible to model the fluid-structure domain, a consistent mass idealization is in most cases desirable.

3. TIME INTEGRATION

In ADINA, the central difference method is employed in explicit time integration and the Newmark method or the Wilson-θ method can be used in implicit time integration[6]. Using implicit time integration a lumped or consistent mass matrix can be employed, but in explicit time integration only a lumped mass idealization can be specified. Table 1 in [7] summarizes the complete solution algorithm employed.

The stability and accuracy characteristics and the computational details of using these techniques in linear analysis have been summarized in [6]. Considering general nonlinear analysis the main difficulty is to assure the stability of a time integration solution. In explicit time integration the solution is simply marched forward, and it may be difficult to identify an instability that manifests itself only as a significant error accumulation over a few time steps. On the other hand, using an implicit time integration method, in each time step the incremental equilibrium equations are solved and equilibrium iterations can be performed on the solution quantities. These equilibrium iterations are equivalent to an energy balance check and can be very important to assure a stable and accurate solution (see sample problem 4.4).

4. SAMPLE SOLUTIONS

The sample analyses presented in this section have been performed using the computer program ADINA in which the fluid elements discussed in this paper have been implemented.

4.1 *Analysis of rigidly-contained water column*

A simple axisymmetric water column idealized using 4-node elements as shown in Fig. 4 was analyzed for a step pressure applied at its free end. Lumped and consistent mass idealizations were employed in this analysis, and the objective was to study the accuracy with which the response of the water column is predicted.

Figure 4 shows the calculated longitudinal displacements at the free end of the column and compares these displacements with the analytical solution. It is seen that using implicit time integration (Newmark method) the free-end displacements in the consistent mass analysis were predicted accurately for a time period that included 6 wave reflections, whereas the lumped mass analysis results are inaccurate.

Because of the simplicity of the problem the method of characteristics shows that in this analysis the exact solution can be calculated using the central difference explicit solution method[11]. To obtain the exact solution the pressure and lumped mass idealizations must be such that the displacements are uniform over the column cross section and $\Delta t = \Delta L/c$, where c is the wave velocity and ΔL is the length of an element.

4.2 *Static analysis of an assemblage of concentric fluid-filled cylinders*

Five concentric fluid-filled cylinders were analyzed for a load applied on a stiff cap. This same problem was studied by Munro and Piekarski[12]. Figure 5 shows the finite element model employed and the predicted fluid pressures. The finite element solution is compared with the approximate analysis results of Munro and Piekarski.

4.3 *Transient analysis of a water-filled copper tube*

The dynamic response of a water-filled copper tube subjected to an impact loading was analyzed. The structure, the loading and the finite element model employed are shown in Fig. 6. This problem was also analyzed by Walker and Phillips[13], who established governing differential equations based on a number of assumptions and solved these equations using the method of characteristics.

Two finite element analyses were performed: a lumped mass and a consistent mass idealization was used. The mass allocation employed in the lumped mass analysis is

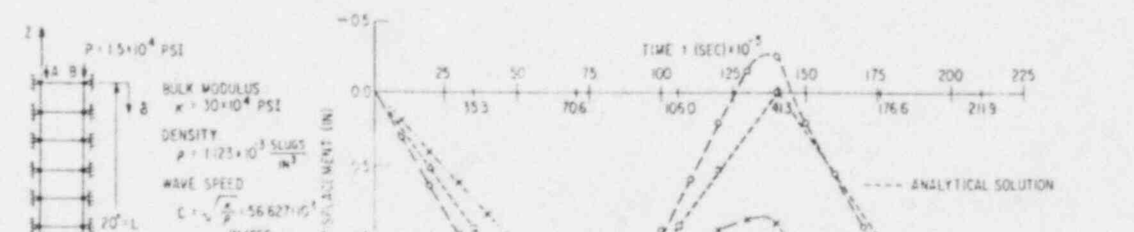

Fig. 4. Longitudinal displacement of free end of rigidly contained water column under pressure step load.

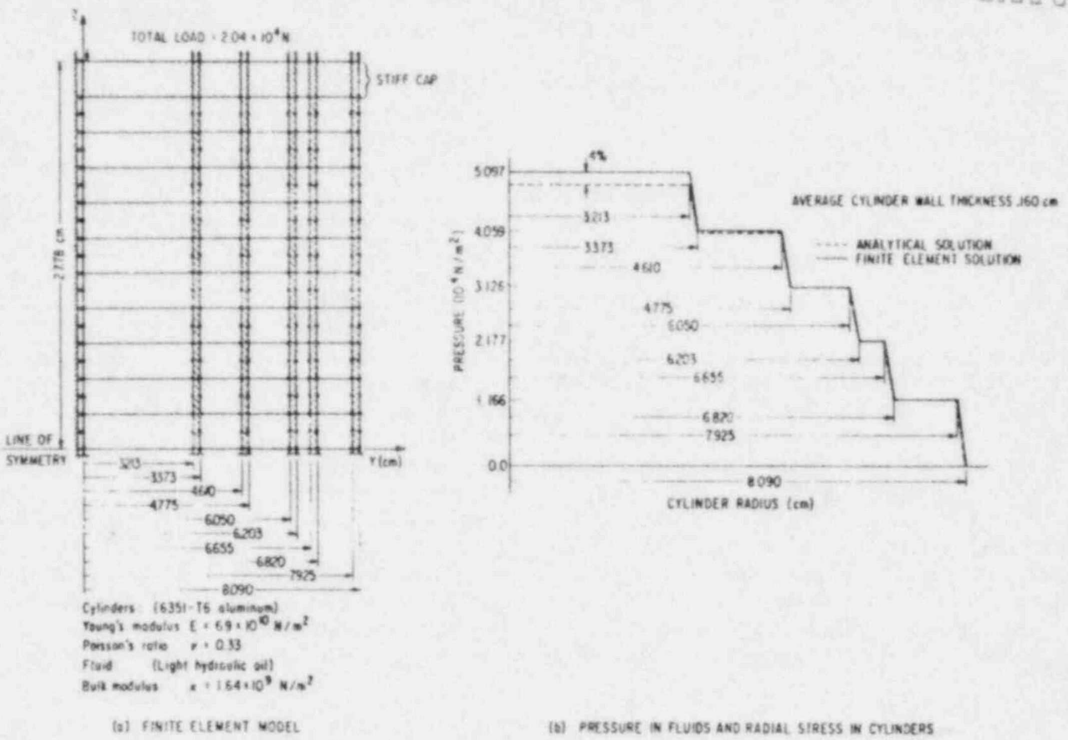

Fig. 5. Static analysis of fluid-filled concentric cylinders.

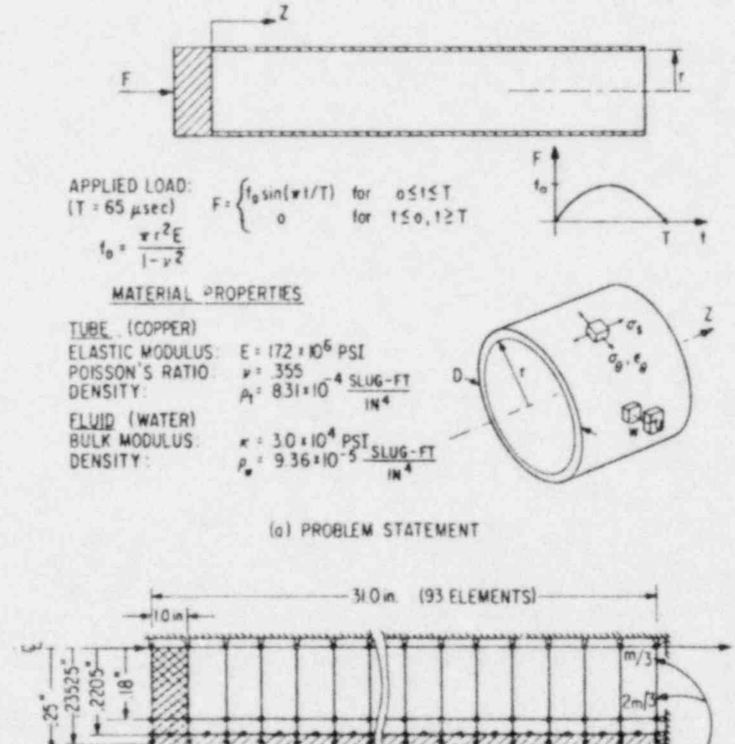

Fig. 6. Analysis of water-filled copper tube.

shown in Fig. 6. This distribution of mass corresponds to the assumption used by Walker and Phillips. It should be noted that a thin layer of elements was used at the tube wall in order to "release" the axial displacements of the fluid.

In both finite element analyses the Newmark method was employed with a time step 1 μsec, i.e. 65 time steps correspond to the pulse length. The length of the elements (axial direction) was about 1/10th of the pulse length. The aspect ratio of the elements was very high (1:34).

Figures 7 and 8 show the response of the system at $Z = 5$in (see Fig. 6) as predicted in this study and by Walker and Phillips. It is seen that for $t < 100\ \mu$sec the finite element solutions correspond reasonably well with the results of Walker and Phillips, but relatively large solution discrepancies are observed at larger times. These solution discrepancies are due to the different assumptions employed in the analyses. Since no experimental or "exact analytical" results are available, it is difficult to assess the actual accuracy of the different models. However, considering the finite element solution results it is seen that the consistent mass model predicts a somewhat smoother response for the hoop strain than does the lumped mass model and gives also results that compare somewhat better with the response predicted in [13].

4.4 *Nonlinear transient analysis of a pipe test*

The experience gained in the above analysis was used to analyze the water-filled straight piping configuration show in Fig. 9 subjected to a pressure pulse at its end. The elastic-plastic response of this pipe was experimentally assessed as reported in [14]. Figure 9 shows also the finite element model employed in the analysis.

In this analysis, a consistent mass matrix was employed and the time integration was carried out using the Newmark method. The time step was changed to half its size at the time the pulse entered the nickel pipe so that the pulse front would pass through a solid element in about three time steps. The effective stiffness matrix used in this analysis was reformed only at time $t = 1.905$, 2.302, and 3.435 msec. However, to take into account the elastic-plastic response of the pipe, equilibrium iterations were used at each time step once the pulse reached the nickel pipe. The equilibrium iterations (energy balance check) were found to be necessary for a stable solution although an average of only 1 to 2 iterations per time step were carried out.

Figure 10 shows the calculated pressures and hoo

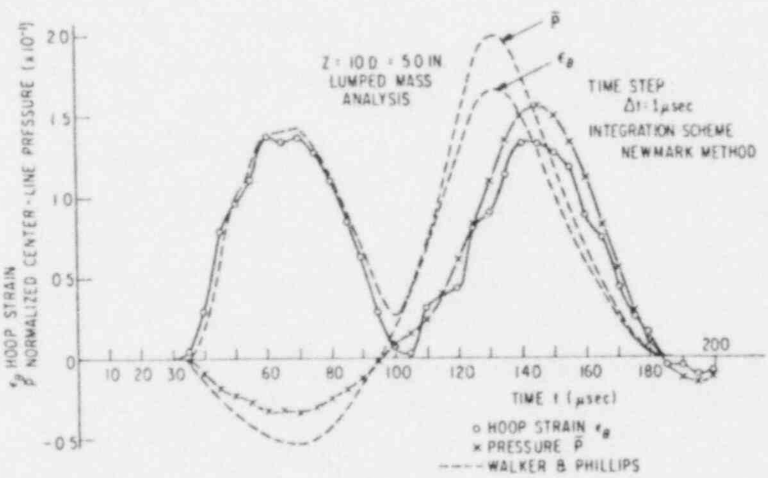

Fig. 7. Response of water-filled copper tube to half sine pulse of 65 μsec duration.

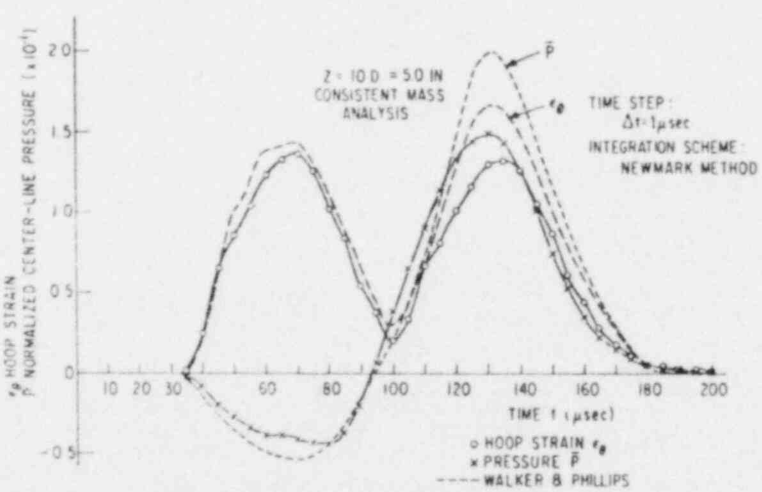

Fig. 8. Response of water-filled copper tube to half sine pulse of 65 μsec duration.

POOR ORIGINAL

POOR ORIGINAL

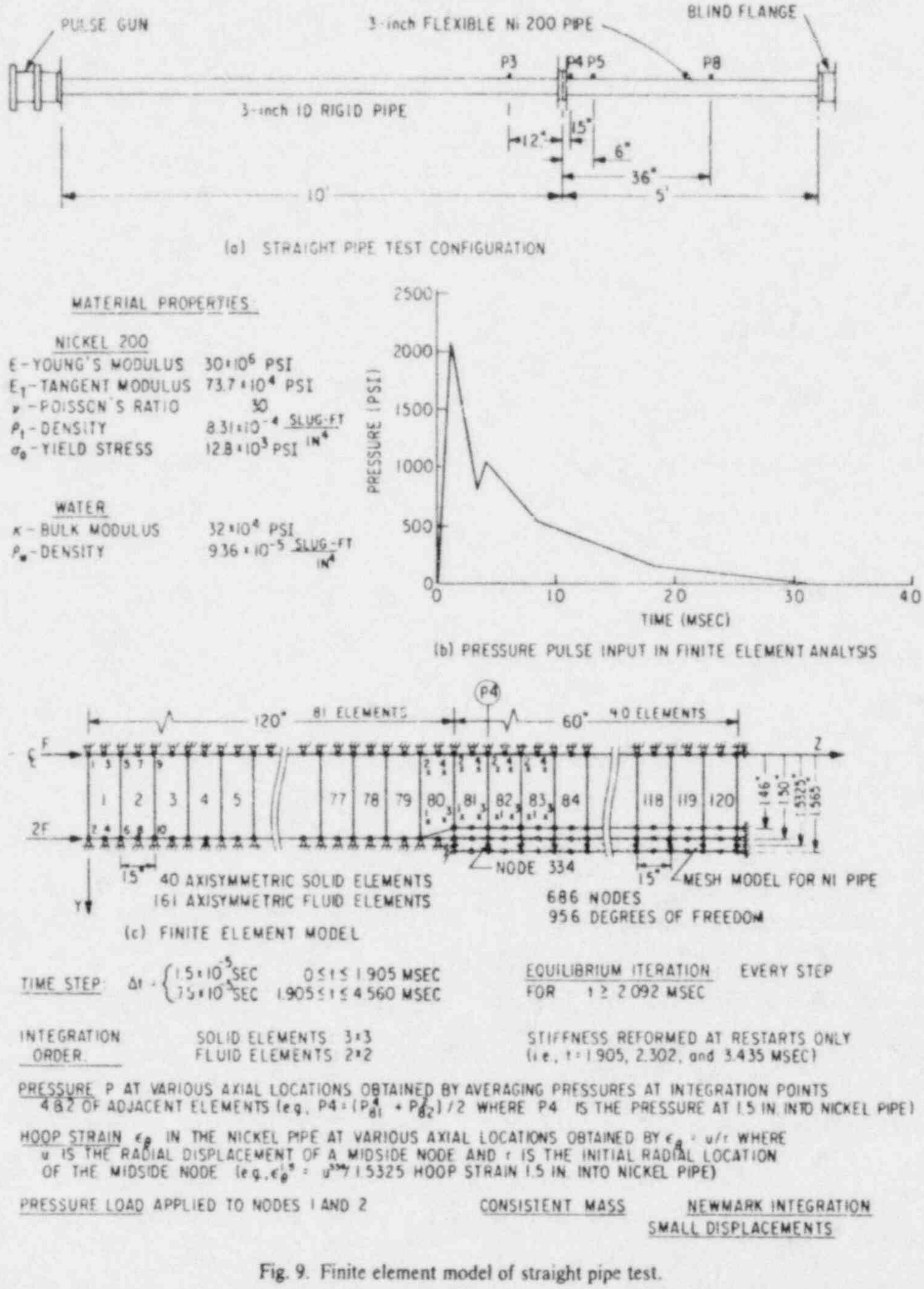

Fig. 9. Finite element model of straight pipe test.

strains at various locations along the pipe as a function of time and compares the ADINA results with the experimental data. It is noted that in general the calculated response compares well with the experimentally observed response.

5. CONCLUSIONS

The transient analysis of fluid-structure systems presents a great deal of difficulties because an appropriate structural and fluid representation together with effective numerical procedures must be employed. In this paper, the fluid is assumed to be inviscid and compressible, an updated Lagrangian formulation is used to describe the fluid motion, isoparametric finite element discretization is employed with lumped or consistent mass idealizations and the incremental equilibrium equations are solved using explicit or implicit time integration. The solution capabilities have been implemented in the ADINA computer program, and the solution results of various sample analyses are presented.

The study performed here indicates that higher-order isoparamatric finite elements can be effective in the representation of the fluid. Depending on the discretization used, the elements may have to be employed with a consistent mass idealization and implicit time integration.

Considering nonlinear analysis, it can be important that equilibrium iterations be performed in order to prevent solution instability. In some analyses only very few iterations are needed to greatly improve the solution accuracy (see Section 4.4).

Since there does not exist a single analysis approach

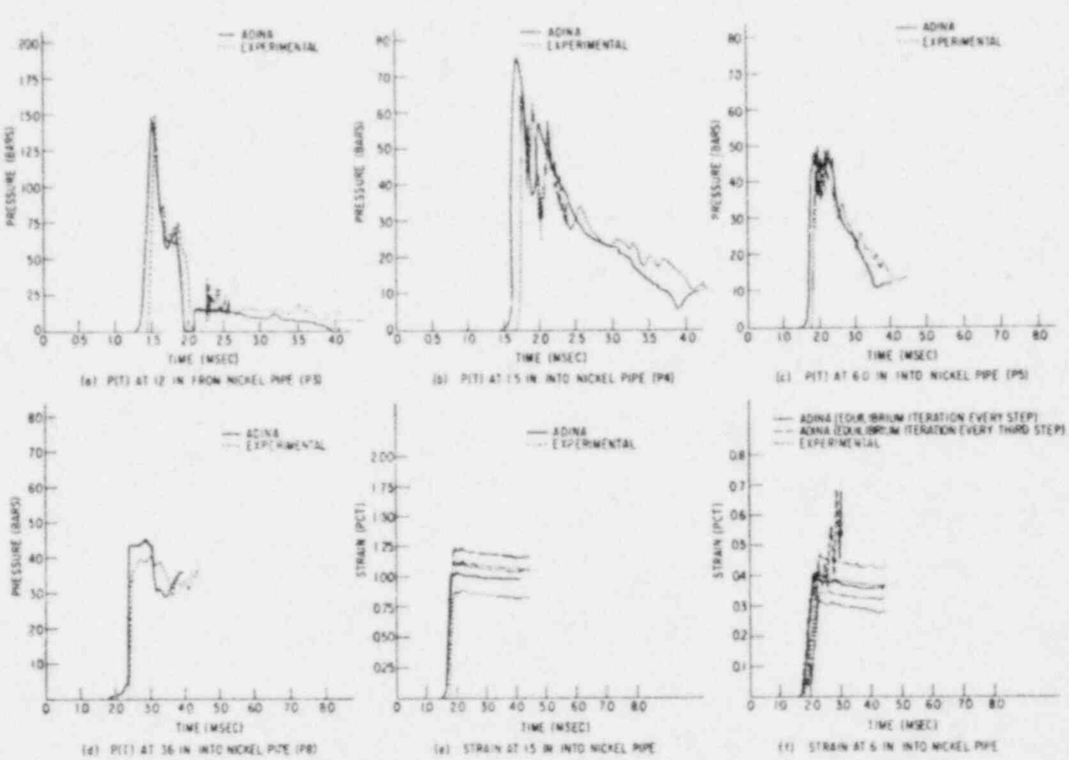

Fig. 10. Pulse propagation in water filled straight pipe system.

that is always most effective for the analysis of fluid-structure problems, it is deemed best at this time to have versatile computational capabilities available. This way, different finite element discretizations, mass idealizations and time integration procedures can be chosen for an effective solution to a particular problem. In this paper much emphasis has been placed on the use of higher-order isoparametric finite elements, consistent mass idealization and implicit time integration. However, it need be noted that these techniques have been employed primarily in two-dimensional analysis and can be prohibitively expensive in three-dimensional response calculations.

Acknowledgements—The work reported in this paper has been supported financially by the Nuclear Regulatory Commission contract No. AT(49-24)-0366 and the ADINA users group. We would like to acknowledge gratefully this support.

REFERENCES

1. T. Belytschko, Methods and programs for analysis of fluid-structure systems. *J. Nuclear Engng and Design* **42**, 41–52 (1977).
2. T. Belytschko, *Transient Analysis, Structural Mechanics Computer Programs* (Edited by W. Pilkey *et al.*), pp. 255–275. University Press of Virginia (1974).
3. J. M. Kennedy and T. Belytschko, Energy source and fluid representation in a structural response code—STRAW. Argonne Natl Lab. *Rep. ANL*-8140 (May 1975).
4. U. W. Chang and J. Gvildys. REXCO-HEP: A two-dimensional computer code for calculating the primary system response in fast reactors. Argonne Natl Lab. *Rep. ANL*-75-19 (June 1975).
5. R. Hofmann, STEALTH, A Lagrangian explicit finite difference code for solids, structural and thermohydraulic analysis. *Electric Power Res. Instit.* Vol. 1–4, Palo Alto, California (June 1976).
6. K. J. Bathe and E. L. Wilson, *Numerical Methods in Finite Element Analysis*. Prentice-Hall, Englewood Cliffs, New Jersey (1976).
7. K. J. Bathe, ADINA-A finite element program for automatic dynamic incremental nonlinear analysis. Acoustics and Vibration Lab., *Rep.* 82448-1, Department of Mechanical Engineering, M.I.T. (Sept. 1975, revised May 1977).
8. K. J. Bathe, E. Ramm and E. L. Wilson, Finite element formulations for large deformation dynamic analysis. *Int. J. Num. Meth. Engng* **9**, 353–386 (1975).
9. L. E. Malvern *Introduction to the Mechanics of a Continuous Medium*. Prentice-Hall, Englewood Cliffs, New Jersey (1969).
10. K. J. Bathe, Static and dynamic geometric and material nonlinear analysis using ADINA. Acoustics and Vibration Lab., *Rep.* 82448-2, Dept. of Mechanical Engng, M.I.T. (May 1976, revised May 1977).
11. S. H. Crandall, *Engineering Analysis-A Survey of Numerical Procedures*. McGraw-Hill, New York (1956).
12. M. Munro and K. Piekarski, Stress-induced radial pressure gradients in liquid-filled multiple concentric cylinders. *J. App. Mech.* **44**(2) 218–221 (1977).
13. J. S. Walker and J. W. Phillips, Pulse propagation in fluid-filled tubes. *J. Appl. Mech.* **44**(1), 31–35 (1977).
14. C. M. Romander, D. J. Cagliostro and A. L. Florence, Experiments on the response of flexible piping systems to internal pressure pulses. SRI *Project PVD*-1960, Stanford Research Institute, Menlo Park, California (April 1976).

Users Manual of Three-dimensional Fluid Element

XXII. 3/D FLUID ELEMENTS

3/D FLUID elements are 8- to 21-node isoparametric or subparametric curvilinear hexahedra. Typical elements are illustrated in Fig. XXII.1.

The following input is required for each element group consisting of 3/D FLUID elements:

Section XXII.1: Element Group Control Card
This card defines the type of 3/D elements in this group, i.e., whether the elements are linear or nonlinear elements.

Section XXII.2: Material Property Data Cards
The stress-strain relations of all elements in this element group must be described by a material model. However, input any number of material property sets (each one defining different material constants) for the specific material model of this group.

Section XXII.3: Element Data Cards
In this section the elements of this group are defined by input of their nodal points, etc.

A specific element group defined by the above input cards is followed by the input cards of another element group (use a 3/D fluid element group, if 3/D fluid elements are still to be input). After all element groups have been defined, proceed to Section XXXI.

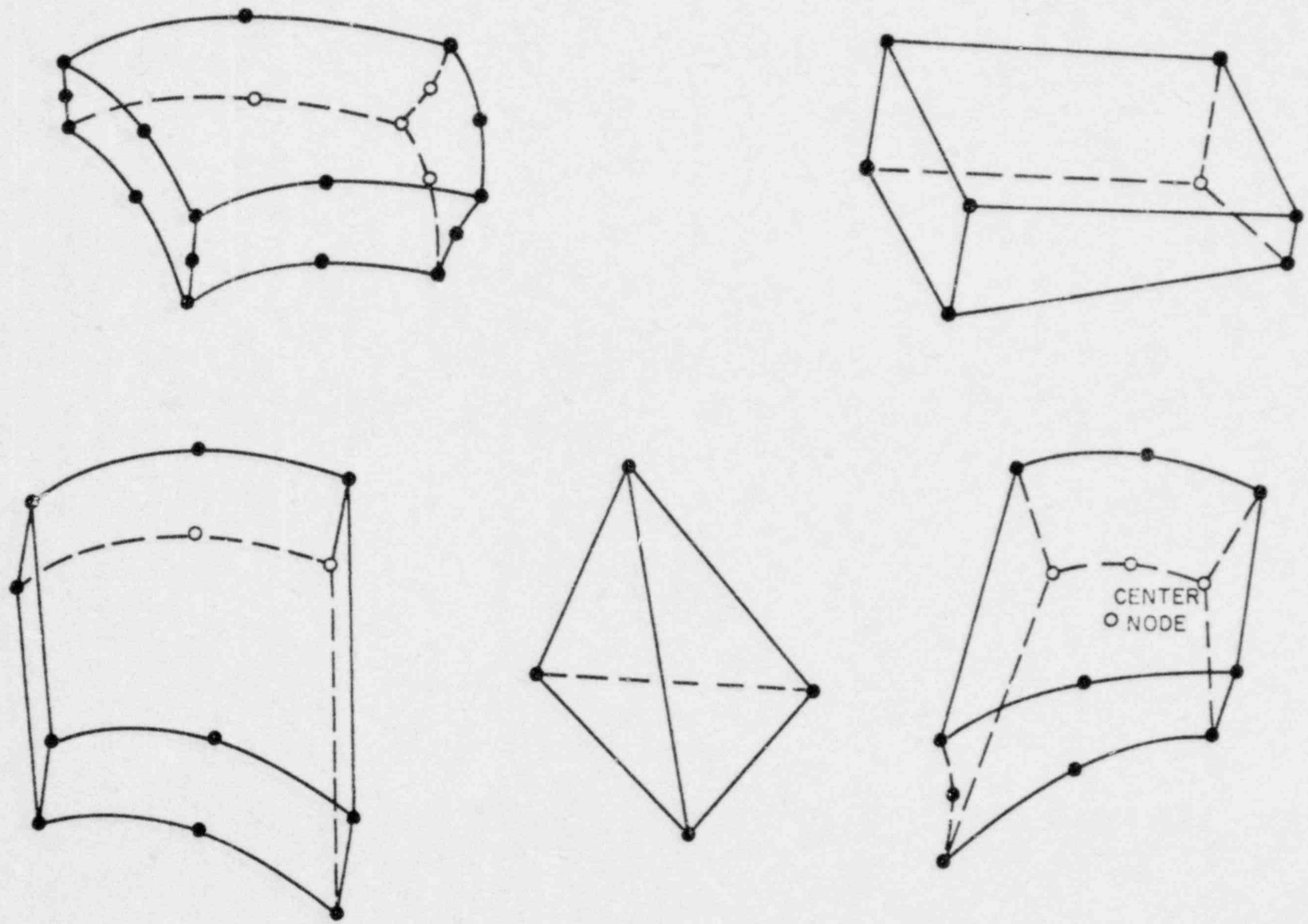

FIGURE XXII.1 TYPICAL 3/D FLUID ELEMENTS DERIVED FROM THE GENERAL ELEMENT IN FIGURE XXII.2

XXII. 3/D FLUID ELEMENTS (continued)

1. Element Group Control Card (2014)

note	columns	variable	entry
	1 - 4	NPAR(1)	Enter the number "12"
(1)	5 - 8	NPAR(2)	Number of 3/D FLUID elements in this group; GE.1
(2)	9 - 12	NPAR(3)	Flag indicating type of nonlinear analysis; EQ.0; linear analysis EQ.1; updated Lagrangian
(3)	13 - 16	NPAR(4)	Element birth and death option; EQ.0; elements are active throughout solution EQ.1; elements become only active at the time of birth EQ.2; elements become inactive at the time of death
(4)	21 - 24	NPAR(6)	Skew coordinate system reference indicator; EQ.0; all element nodes use the global system only EQ.1; some element node degrees-of-freedom are referred to a skew coordinate system
(5)	25 - 28	NPAR(7)	Maximum number of nodes used to describe any one element; EQ.0; default set to "21"
(6)	37 - 40	NPAR(10)	Numerical integration order to be used in Gauss quadrature formula for r-s plane; EQ.0; default set to "2" GE.2 and LE.4
(6)	41 - 44	NPAR(11)	Numerical integration order to be used in Gauss quadrature formula for t-direction; EQ.0; default set to "2" GE.2 and LE.4

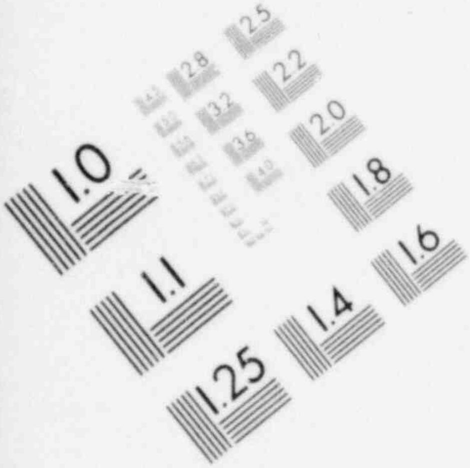

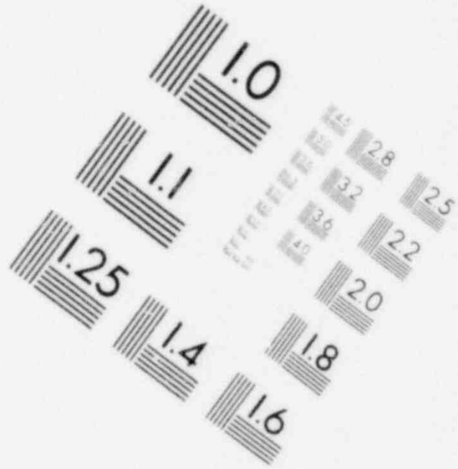

IMAGE EVALUATION TEST TARGET (MT-3)

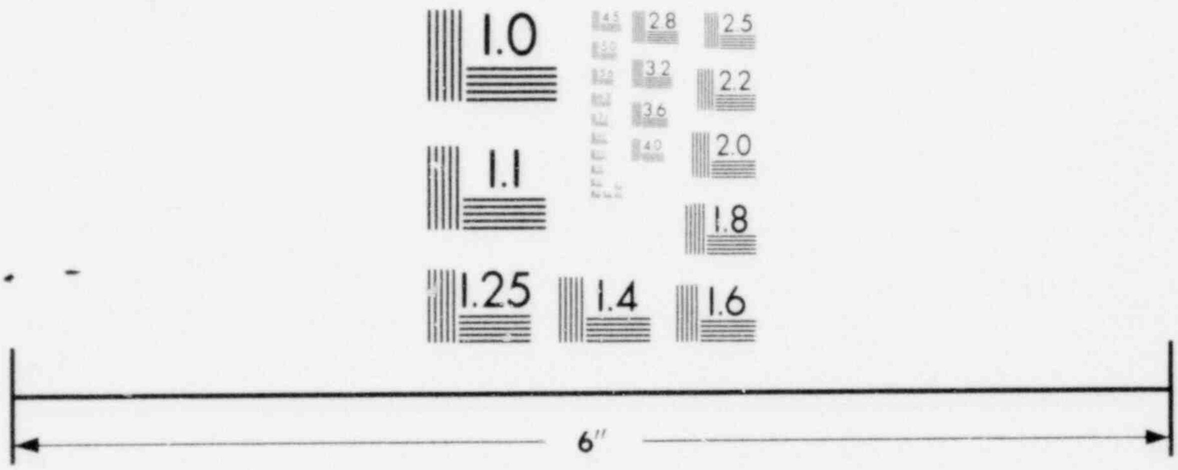

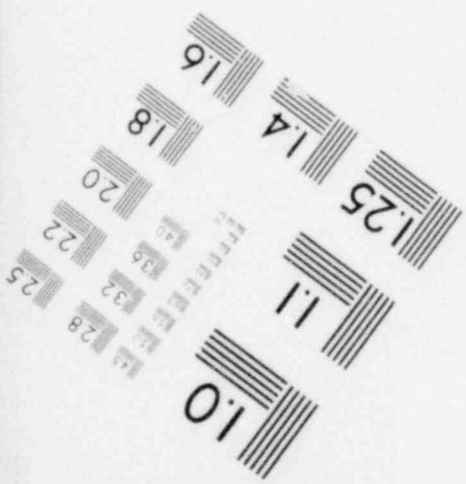

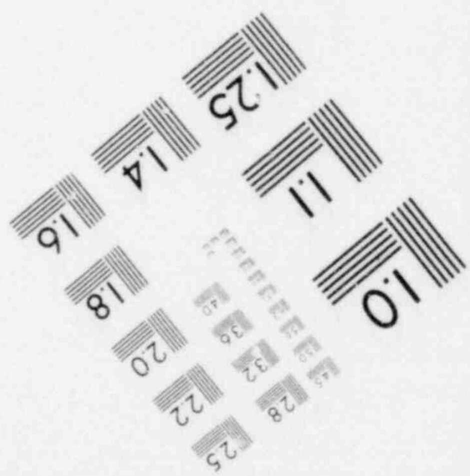

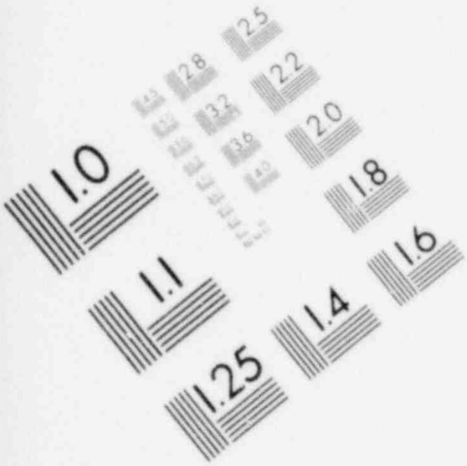

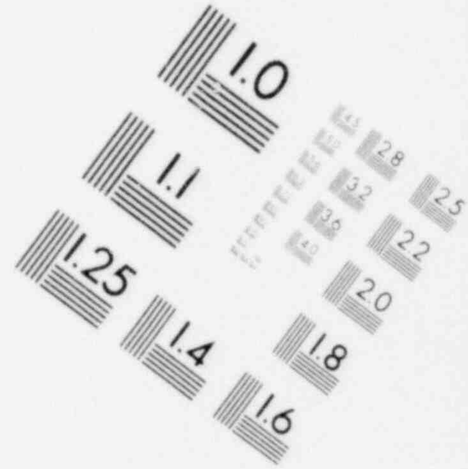

IMAGE EVALUATION TEST TARGET (MT-3)

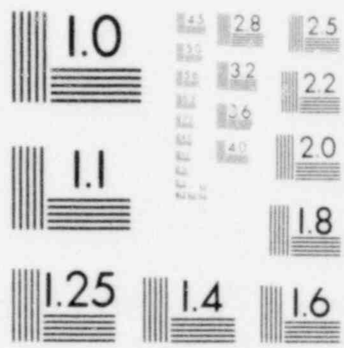

6″

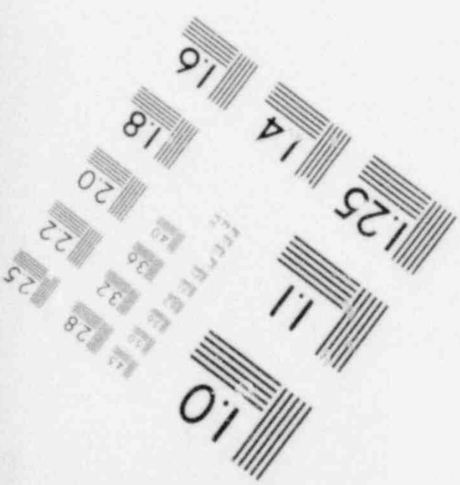

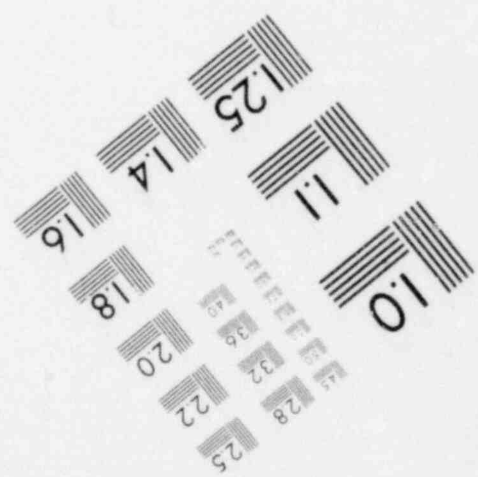

XXII. 3/D FLUID ELEMENTS (continued)

note	columns	variable	entry
(7)	57 - 60	NPAR(15)	Material model number; EQ.0 ; default set to "1" EQ.1 ; inviscid compressible fluid with constant bulk modulus
(8)	61 - 64	NPAR(16)	Number of different sets of material properties; GE.1
(3)	65 - 68	NPAR(17)	Number of constants per material property set; EQ.0; if NPAR(15).EQ.1

NOTES/

(1) 3/D FLUID element numbers begin with one (1) and end with the total number of elements in this group, NPAR(2). Data for the individual elements are input in Section XXII.3.

(2) NPAR(3) is applicable to linear and nonlinear element groups and determines the type of nonlinearities to be considered in the analysis.

(3) The variable NPAR(4) identifies whether the elements of the element group are active throughout the solution. The element birth and death option can only be used in a non-linear element group, i.e. if NPAR(3).GT.0, NPAR(4) can take three different modes:

(i) If NPAR(4).EQ.0, the elements are active throughout the solution (this is the usual case, in which no material is added or removed from the physical system).

(ii) If NPAR(4).EQ.1, the elements are not active until a specific solution time. The solution time at which an element becomes active (ETIME) is input on the element card (see Section XXII.3).

It should be noted that prior to the time at which a specific element becomes active, the nodal points to which the element is connected have, in general, displaced. In the analysis, the stress-free configuration of an element is defined to be the element configuration at the time at which the element becomes active. In other words, the nodal displacements that occurred prior to the time at which the element becomes active are assumed to cause no stresses in the element.

XXII. 3/D FLUID ELEMENTS

NOTES/

(3) (continued)

(iii) If NPAR(4).EQ.2, the elements are initially active but become inactive at a specific solution time. The solution time at which an element becomes inactive (ETIME) is input on the element card (see Section XXII.3).

It should be noted that the element birth and death options are only applicable to the element stiffness matrices, i.e. the removal or addition of an element only alters the global stiffness matrix of the complete element assemblage. The mass matrix is always constructed corresponding to the total and complete element assemblage, i.e. all elements are assumed to be active. Since the element birth and death option can only be used in a nonlinear material description, which can be employed in conjunction with any of the linear or nonlinear material models.

(4) The variable NPAR(6) indicates whether the degrees-of-freedom at some of the nodes of the elements defined in this group are referred to a skew coordinate system (see Section V.1 for definition of the skew coordinate system). If skew coordinate systems are used and a large finite element system is analyzed, it is most efficient to put all element that use nodes with skew coordinate systems into one (or more) element groups, i.e., for solution effectiveness all elements in this element group should have nodes with skew coordinate systems if NPAR(6).EQ.1.

(5) NPAR(7) is the maximum number of nodes that can be used to describe any one of the elements in this group, i.e. elements in this group must have less than or equal to NPAR(7) nodes. A minimum of 8 and a maximum of 21 nodes are used to describe 3/D FLUID elements as indicatedin Fig. XXII. Constant strain tetrahedra can be formed from 8-node elements by having nodes 1, 2, 3, and 4 coincide and nodes 7 and 8 coincide.

(6) The selection of appropriate integration orders depends on the element shape and strain state being considered. When the quantities being integrated vary irregularly a higher order is needed. An integration order of "2" is sufficient for most problems. Shell or plate problems often use thin elements in which strain varies more or less linearly through the thickness, but more irregularly in the plane of the surface of the shell. In these cases it is advantageous to specify a lower order for integration through the thickness, i.e., NPAR(11) < NPAR(10).

The expense of stiffness formation is dependent on the integration order, i.e.,

$$n = NPAR(11) * NPAR(10) * NPAR(10)$$

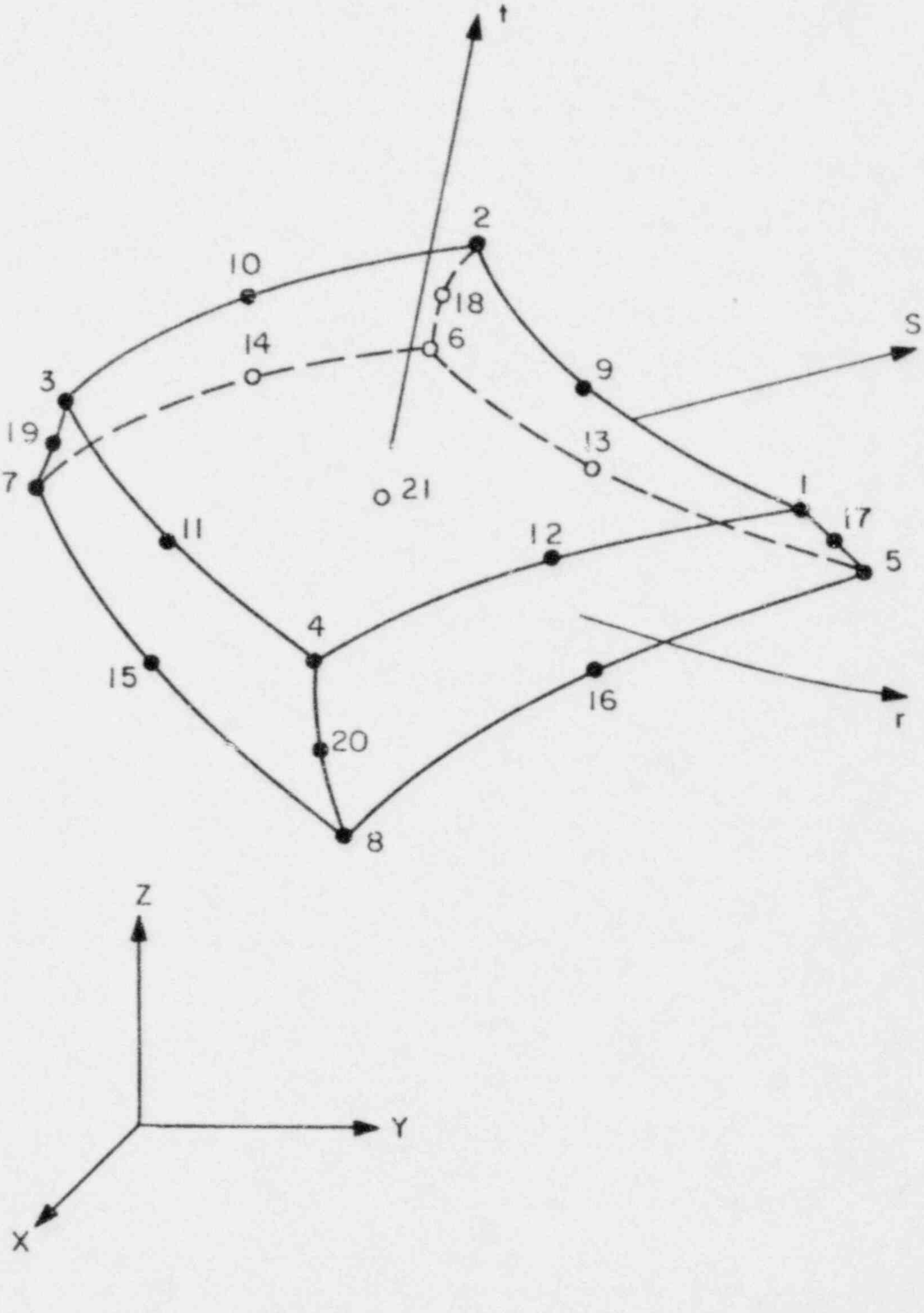

FIGURE XXII.2 3/D FLUID ELEMENT NODE NUMBERING CONVENTION

NOTES/

(6) (continued)

where n is the number of points at which $\underline{B}^T \underline{C}\,\underline{B}$ must be calculated in order to find the element stiffness by Gauss integration.

The consistent mass matrix is always calculated using an integration order of three in each direction.

(7) Only one material model (defined by the value of NPAR(15)) is allowed in an element group. Currently only a material with a constant bulk modulus can be assumed.

2. Material Property Data Cards

NPAR(16) sets of cards must be input in this section.

a. material number card (I5,F10.0)

note	columns	variable	entry
	1 - 5	N	Material property set number GE.1 and LE.NPAR(16)
(1)	6 - 15	DEN(N)	Mass density of the material used in the calculations of the mass matrix; GE.0.0

NOTES/

(1) The mass density defined is used directly in the calculation of the element mass matrix, i.e. no acceleration constants are applied to the varible DEN(N). The mass density is also employed in the calculation of the gravity load vector (see Note (3), Section V).

b. material property card(s) (8F10.0)

For MODEL "1" (NPAR(15).EQ.1 → [Inviscid linear elastic]

note	columns	variable	entry
(1)	1 - 10	PROP(1,N)	Bulk modulus, K

NOTES/

(1) MODEL 1 is a linear library model defined by one (1) positive constant (K); i.e., if NPAR(15).EQ.1, NPAR(17) is set to "1" by default. MODEL 1 can be used with linear or nonlinear element groups.

XXII. 3/D FLUID ELEMENTS (continued)

3. Element Data Cards

Three cards must be prepared for each element that appears in the input:

Card 1 (7I5,F10.0)

note	columns	variable	entry
(1)	1 - 5	M	3/D FLUID element number; GE.1 and LE.NPAR(2)
(2)	6 - 10	IELD	Number of nodes to be used in describing the element's displacement field; EQ.0, default set to NPAR(7) LE.NPAR(7)
(3)	11 - 15	IELX	Number of nodes to be used in the description of the element's geometry; EQ.0; default set to IELD GE.8 and LE.IELD EQ.IELD → isoparametric element EQ.IELD → subparametric element
(4)	16 - 20	IPS	Flag for printing pressures; EQ.0; no pressure output for this element EQ.1; print pressures at integration points
	21 - 25	MTYP	Material property set number assigned to this element; GE.1 and LE.NPAR(16)
(5)	26 - 30	IST	Flag indicating that the stiffness and mass matrices for this element are the same as those for the preceding element; EQ.0; no EQ.1; yes

XXII. 3/D FLUID ELEMENTS (continued)

note	columns	variable	entry
(6)	31 - 35	KG	Node number increment for element data generation; EQ.0 default set to "1"
(7)	36 - 45	ETIME	Time of element birth or death

XXII. 3/D FLUID ELEMENTS (continued)

Card 1 (8I5)

note	columns	variable	entry
(2)	1 - 5	NOD(1)	Global node number of element nodal point 1
	6 - 10	NOD(2)	Global node number of element nodal point 2
	11 - 15	NOD(3)	...
	16 - 20	NOD(4)	
	21 - 25	NOD(5)	
	26 - 30	NOD(6)	
	31 - 35	NOD(7)	
	36 - 40	NOD(8)	Global node number of element nodal point 8

CARD 3 (13I5)

note	columns	variable	entry
(2)	1 - 5	NOD(9)	Global node number of element nodal point 9
	6 - 10	NOD(10)	...
	11 - 15	NOD(11)	
	16 - 20	NOD(12)	
	21 - 25	NOD(13)	

XXII. 3/D FLUID ELEMENTS (continued)

note	columns	variable	entry
	26 - 30	NOD(14)	Global node number of element nodal point 14
	31 - 35	NOD(15)	...
	36 - 40	NOD(16)	
	41 - 45	NOD(17)	
	46 - 50	NOD(18)	
	51 - 55	NOD(19)	
	56 - 60	NOD(20)	
	61 - 65	NOD(21)	Global node number of element nodal point 21

NOTES/

(1) Element cards must be input in ascending element number order beginning with one (1) and ending with NPAR(2). Repetition of element numbers is illegal, but element cards may be omitted, and missing element data generated according to the procedure described in note (6).

(2) IELD is a count of the node numbers actually posted on Cards 2 and 3 which must immediately follow Card 1. IELD must be at least eight (8), but must be less than or equal to the limit NPAR(7) which was given on the Element Group Control Card, Section XXII.1. Element displacements are assigned at the IELD non-zero nodes, and thus the order of the element matrices is three (i.e., translations X,Y, Z) times IELD. The eight corner nodes of the hexahedron must be input, but nodes 9 to 21 are optional, and any or all of these optional nodes may be used to describe the element's displacement field. However, all 21 entries for NOD(1) are read from element data cards 2 and 3; if IELD.LT.21 the particular node locations not used in this element must

NOTES/ (continued)

be input as zero (0) in NOD(I). Figure XXII.2 defines the input sequence that must be observed for element input.

For example, the 10-node element (IELD.EQ.10) shown below

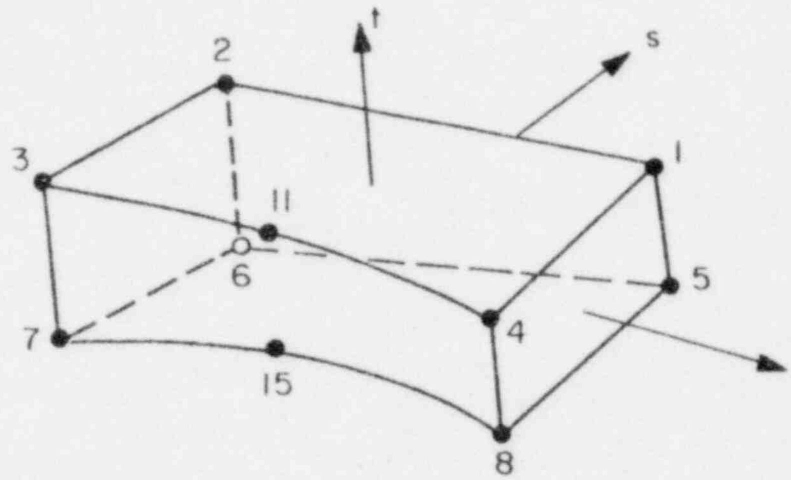

is defined by

NOD(I) = [X X X X X X X X 0 0 X 0 0 0 X 0 0 0 0 0 0],

where the nonzero entries (X) are the global mesh node numbers (Section V) of the 10 nodes.

(3) When the element edges are straight it is unnecessary computationally to include side nodes in the numerical evaluation of coordinate derivatives, the Jacobian matrix, etc., and since such element shapes are common, an option has been included to use fewer nodes in these geometric calculations than are used to describe element displacements. The first IELX nonzero nodes posted on Cards 2 and 3 are used to evaluate those parameters which pertain to element geometry only. IELX must be at least eight (8), and if omitted is re-set to IELD. A common application might be a 20 node element (i.e., IELD.EQ.20) with straight edges in which case IELX would be entered as "8".

(4) If IPS.EQ.0 no pressure output will be provided and saved on the porthole element. To print and save the element pressures, input IPS.EQ.1.

(5) For linear analyses, the flag IST allows the program to bypass stiffness and mass matrix calculations provided the

NOTES/

(5) (continued)

current element is identical to the preceding element; i.e., the preceding and current elements are identical except for a rigid body translation. If ISR.EQ.0, new matrices are computed for the current element. When an out-of-core solution is required or the element is nonlinear, the program automatically calculates stiffness and mass matrices for each element regardless of the value of IST.

(6) When element cards are omitted, element data are generated automatically as follows:

a) All data on Card 1 for generated elements is taken to be the same as that given on the first element card in the sequence;

b) Nonzero node numbers (given on Cards 2 and 3 for the first element) are incremented by the value "KG" (on the first element's Card 1) as element generation progresses; zero (or blank) node number entries are generated as zeroes.

The last element cannot be generated.

(7) The time at which the element becomes active (if NPAR(4).EQ.1), i.e. the time of element birth, or inactive (if NPAR(4).EQ.2), i.e. the time of element death, must be defined if NPAR(4).GT.0 on the Element Group Control Card (see Section XXII.1).

ANALYSIS OF A PLATE WITH FLUID LOADING

The static and dynamic behavior of a square plate loaded with a fluid was analyzed.

One quarter of the plate was modelled using nine 16-node 3-D solid elements. The fluid above the plate was modelled using three layers of 3-D fluid elements. The layer immediately above the plate consists of nine 12-node elements and the two layers above it were each made up of nine 8-node elements. The dimensions and material properties of the plate and fluid are shown in Figure 1.

(a) Static Analysis

The plate was fully supported at the bottom, and both the plate and the fluid were constrained from lateral movement at the edges, while the internal nodes were left free. A uniform pressure applied in the vertical direction resulted only in vertical displacements of the nodes. The pressure is transmitted uniformly throughout the fluid while the plate develops stresses in the x,y,z directions which agree with theoretical values.

(b) Frequency Analysis

The plate was simply supported and free to move in the transverse direction while the fluid is constrained to move vertically. The natural frequency of vibration of the plate was determined with and without the fluid -- and the results for the first three modes are shown in

Figure 1. It is seen that the presence of the fluid reduces the frequency of vibration of the plate by about 15% in these models. However, a considerably finer mesh would be required to model the dynamic behavior accurately.

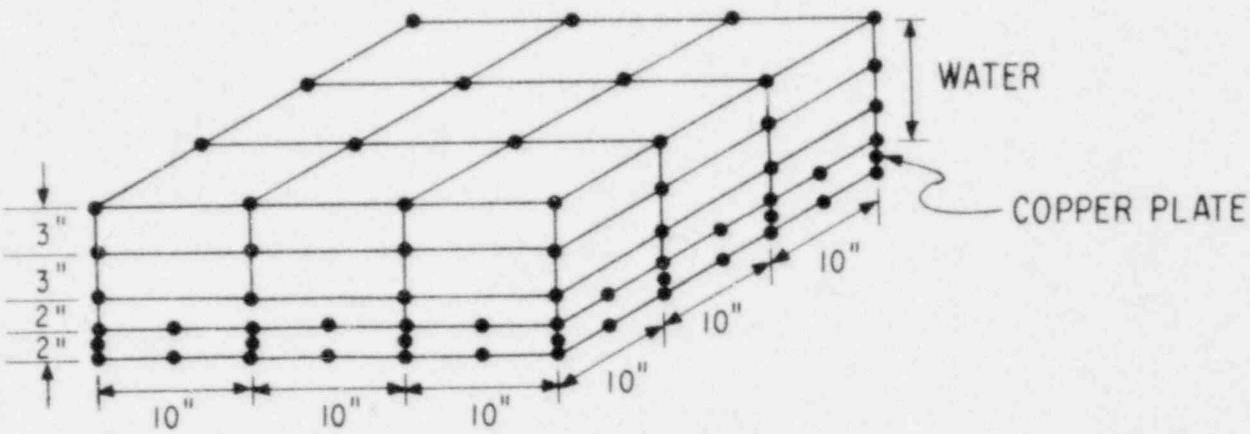

COPPER

YOUNG'S MODULUS = 17.2×10^6 P.S.I.
POISSON'S RATIO = 0.355
DENSITY = 0.831×10^{-3} SLUG FT/IN^4

WATER

BULK MODULUS = 30×10^4 P.S.I.
DENSITY = 0.936 SLUG FT/IN^4

	FREQUENCY IN RADIANS / SECOND	
MODE NO.	PLATE ALONE	PLATE WITH FLUID
1	0.58×10^3	0.49×10^3
2	2.95×10^3	2.46×10^3
3	2.95×10^3	2.46×10^3

FIG. 1 FINITE ELEMENT MODEL OF PLATE AND FLUID

NRC FORM 335 (7-77)

U.S. NUCLEAR REGULATORY COMMISSION

BIBLIOGRAPHIC DATA SHEET

4. TITLE AND SUBTITLE (Add Volume No., if appropriate) A Three-Dimensional Fluid Finite Element	1. REPORT NUMBER (Assigned by DDC) NUREG/CR-1232
	2. (Leave blank)
	3. RECIPIENT'S ACCESSION NO.
7. AUTHOR(S) K. J. Bathe, W. F. Hahn	5. DATE REPORT COMPLETED MONTH July YEAR 1979
9. PERFORMING ORGANIZATION NAME AND MAILING ADDRESS (Include Zip Code) Massachusetts Institute of Technology Cambridge, Massachusetts 02139	DATE REPORT ISSUED MONTH January YEAR 1980
	6. (Leave blank)
	8. (Leave blank)
12. SPONSORING ORGANIZATION NAME AND MAILING ADDRESS (Include Zip Code) U. S. Nuclear Regulatory Commission Office of Nulcear Reactor Regulation Division of Project Management Washington, D. C. 20555	10. PROJECT/TASK/WORK UNIT NO.
	11. CONTRACT NO. NRC-03-78-142
13. TYPE OF REPORT Technical	PERIOD COVERED (Inclusive dates) October 1, 1978-September 30, 1979
15. SUPPLEMENTARY NOTES	14. (Leave blank)

16. ABSTRACT (200 words or less)

A three-dimensional fluid finite element compatible with the solid elements in the ADINA finite element program has been developed for the analysis of wave propagation in fluid and fluid-structural systems. The fluid element can model inviscid compressible fluids with constant bulk modulus. Although the final discretized equations of motion are valid for general loading and displacement conditions, the numerical computations only admit relatively small fluid displacements unless mesh rezoning would be used.

17. KEY WORDS AND DOCUMENT ANALYSIS	17a. DESCRIPTORS
17b. IDENTIFIERS/OPEN-ENDED TERMS	

18. AVAILABILITY STATEMENT NO RESTRICTIONS ON AVAILABILITY	19. SECURITY CLASS (This report) Unclassified	21. NO. OF PAGES
	20. SECURITY CLASS (This page) Unclassified	22. PRICE $

NRC FORM 335 (7-77)